Discussion

This is the first clinical investigation to explore the expression of AQP4 and AQP5 in LSGs from patients with pSS or NMOsd-SS. We obtained the following new results.

First, although AQP4 is considered to be a major autoantigen in patients with NMOsd, AQP4 was not expressed in the LSGs of our four NMOsd-SS patients. In addition, AQP4 was not expressed in LSGs from the eight pSS patients or the three control subjects. The extensive loss of AQP4 immunoreactivity is reported in the demyelinated plaques in spinal cord of patients with NMO,[27] indicating that AQP4 expressed in the target organs of NMO may be destroyed by anti-AQP4 autoantibodies. In the present study, since AQP4 was not expressed in the LSGs from the control subjects, SS and NMO-SS, AQP4 appears not to be involved in the chronic sialadenitis of NMOsd-SS as well as pSS.

Second, we found that an abnormal distribution of AQP5 in LSGs may be associated with poor saliva secretion. A previous study revealed that AQP5 is distributed in salivary glands, bronchial glands and lacrimal glands and functions as a water channel in secretary glands, lung, and eye.[28] Steinfeld et al.[20] reported the same abnormal distribution of AQP5 as that observed in the LSGs of the present study's pSS patients. Since the expression ratio of AQP5 on the apical side of acini was even lower in our study's group with poor saliva secretion, our data may strengthen the speculation that AQP5 is a major water channel involved in the salivary secretory function of SS. We observe differences between AQP5 distribution in Table 2 and results from Saxon test. With respect to these differences, we should note the presence of other factors including humoral factors, apoptosis-related molecules and inflammatory cytokines that affect the salivation because these factors might influence on distribution of AQP5. Factors such as epidermal growth factor to promote salivary secretion by protecting the salivary glands from cell death might also have potential to effect on AQP 5 trafficking. An abnormal distribution of AQP5 was also observed in the lacrimal glands by Tsubota et al.,[29] suggesting that the trafficking of AQP5 in exocrine glands may be common in patients with SS.

Third, although the histological similarity of LSG pathology between pSS and NMOsd-SS is strongly suggested, a difference might also exist since the abnormal AQP5 distribution in LSGs tended to be prominent in our NMOsd-SS patients compared to those with pSS. Different from LSGs from SS patients, specific factors found in NMO might influence on AQP5 distribution detected in LSGs from the patients with NMOsd-SS. In addition, the infiltration of MNCs into LSGs was less in the NMOsd-SS patients. These data may indicate the presence of some humoral factors involved specifically in the chronic sialadenitis of patients with NMOsd-SS. In addition,

we should note the limitation of analysis for saliva secretion with regard to the group of NMOsd-SS. Because complication of NMOsd and SS is considered to be relatively rare, inadequate and inaccurate statistical analysis might occur for this cluster in the present analysis.

In this regard, we examined the expression of TNF-α in the LSGs of patients with pSS or NMOsd-SS. The expression of varying cytokines, including TNF-α and IL-10, are found to be elevated in the serum or LSGs of SS patients.[30] Similarly, serum or cerebrospinal fluid concentrations of TNF-α and IL-10 are also elevated in NMO patients.[23,31] In the present study, we did not find a difference in the TNF- α expression in LSGs between the pSS and NMOsd-SS patients. Although Yamamura et al. reported that TNF-α inhibits AQP5 expression in an immortalized human salivary gland acinar cell line via the suppression of histone H4 acetylation,[32] we found that neither TNF-α nor IL-10 altered the expression level of AQP5 in primary SGECs. These data may indicate that TNF-α and/or IL-10 did not change the total amount of AQP5, although effect of these cytokines toward the distribution pattern of AQP5 remains unclear. However, at present, the exact factors or mechanisms that contribute to the abnormal distribution of AQP5 in LSGs found in patients with pSS or NMOsd-SS are not known.

In summary, AQP5 but not AQP4 appears to be involved in the salivary gland dysfunction of patients with pSS or NMOsd-SS. Elucidation of the humoral and/or cellular factors responsible for the unique kinetic changes of AQP5 in these patients is desired.

Acknowledgment

This work was supported in part by a Grant from The Ministry of Health, Labour and Welfare, Japan. We appreciate Cosmic Corporation for the measurement of anti-AQP4 antibody. We also thank Ms Yoshiko Takahashi for her technical assistance.

Conflict of Interest

None

References

1. Mavragani CP, Moutsopoulos HM. Sjögren's syndrome. Annu Rev Pathol 2014;9:273-85.
2. Skopouli FN, Dafni U, Ioannidis JP, Moutsopoulos HM. Clinical evolution, and morbidity and mortality of primary Sjögren's syndrome. Semin Arthritis Rheum 2000;29:296-304.
3. Chai J, Loqiqian EL. Neurological manifestations of primary Sjogren's syndrome. Curr Opin Neurol 2010; 23:509-13.
4. Fauchais AL, Magy L, Vidal E. Central and peripheral neurological complications of primary Sjögren's syndrome. Presse Med 2012;41:485-93.
5. Wingerchuk DM, Lennon VA, Pittock SJ, Lucchinetti CF, Weinshenker BG. Revised diagnostic criteria for neuromyelitis optica. Nerology 2006;66:1485-1489.
6. Wingerchuk DM, Lennon VA, Lucchinetti CF, Pittock SJ, Weinshenker BG. The spectrum of neuromyelitis optica. Lancet Neurol 2007; 6: 805-15.
7. Ghezzi A, Bergamaschi R, Martinelli V, Trojano M, Tola MR, Merelli E et al. Clinical characteristics, course and prognosis of relapsing Devic's neuromyelitis optica. J Neurol 2004; 251: 47-52.
8. Wingerchuk DM, Hogancamp WF, O'Brien PC, Weinshenker BG. The clinical course of neuromyelitis optica (Devic's syndrome). Neurology 1999; 53: 1107-14.
9. Rivera JF, Kurtzke JF, Booth VJ, Corona VT 5th. Characteristics of Devic's disease (neuromyelitis optica) in Mexico. J Neurol 2008;255:710-5.
10. Lim YM, Pyun SY, Lim HT, Jeong IH, Kim KK. First-ever optic neuritis: distinguishing subsequent neuromyelitis optica from multiple sclerosis. Neurol Sci 2014;35:781-3.
11. Tomizawa Y, Yokoyama K, Saiki S, Takahashi T, Matsuoka J, Hattori N. Blood-brain barrier disruption is more severe in neuromyelitis optica than in multiple sclerosis and correlates with clinical disability. J Int Med Res 2012;40:1483-91.
12. Fernandes DB, Ramos Rde I, Falcochio C, Apóstolos-Pereira S, Callegaro D, Monteiro ML. Comparison of visual acuity and automated perimetry findings in patients with neuromyelitis optica or multiple sclerosis after single or multiple attacks of optic neuritis. J Neuroophthalmol 2012;32:102-6.
13. Preston GM, Carroll TP, Guggino WB, Agre P. Appearance of water channels in Xenopus oocytes expressing red cell CHIP28 protein. Science 1992;256:385-7.
14. Aqre P, King LS, Yasui M, Guggino WB, Ottersen OP, Fujiyoshi Y et al. Aquaporin water channels — from atomic structure to clinical medicine. J Physiol 2002;542:3-16.

15. Verkman AS Anderson MO, Papadopoulos MC. Aquaporins: important but elusive drug targets. Nat Rev Drug Discov 2014;13:259-77.
16. Lennon VA, Wingerchuk DM, Kryzer TJ, Pittock SJ, Lucchinetti CF, Fujihara K, et al. A serum autoantibody marker of neuromyelitis optica: distinction from multiple sclerosis. Lancet 2004;364:2106-12.
17. Lennon VA, Kryzer TJ, Pittock SJ, Verkman AS, Hinson SR. IgG marker of optic-spinal multiple sclerosis binds to the aquaporin-4 water channel. J Exp Med 2006;202:473-7.
18. Pittock SJ, Lennon VA, Krecke K, Wingerchuk DM, Lucchinetti CF, Weinshenker BG. Brain abnormalities in neuromyelitis optica. Arch Neurol 2006; 63: 390-6.
19. Bichuetti DB, Oliveira EM, Souza NA, Rivero RL, Gabbai AA. Neuromyelitis optica in Brazil: a study on clinical and prognostic factors. Mult Scler 2009;15:613-9.
20. Steinfeld S, Cogan E, King LS, Aqre P, Kiss R, Delporte C. Abnormal distribution of aquaporin-5 water channel protein in salivary glands from Sjögren's syndrome patients. Lab Invest 2001;81:143-8.
21. Javed A, Balabanov R, Arnason BG, Kelly TJ, Sweiss NJ, Pytel P et al. Minor salivary gland inflammation in Devic's disease and longitudinally extensive myelitis. Multiple Sclerosis 2008; 14: 809-14.
22. Vitali C, Bombardieri S, Jonsson R, Moutsopoulos HM, Alexander EL, Carsons SE et al. Classification criteria for Sjogren's syndrome: a revised version of the European criteria proposed by the American-European Consensus Group. Ann Rheum Dis 2002; 61: 554-8.
23. Chisholm DM, Mason DK. Labial salivary gland biopsy in Sjögren's disease. J Clin Pathol 1968;21:656-60.
24. Greenspan JS, Daniels TE, Talal N, Sylvester RA. The histopathology of Sjögren's syndrome in labial salivary gland biopsies. Oral Surg Oral Med Oral Pathol 1974;37:217-29.
25. Nakamura H, Kawakami A, Ida H, Koji T, Eguchi K. EGF activates PI3K-Akt and NF-kappaB via distinct pathways in salivary epithelial cells in Sjögren's syndrome. Rheumatol Int 2007;28:127-36.
26. N. Ogawa, L. Ping, L. Zhenjun, Y. Takada, S. Sugai, Involvement of the interferon-γ-induced T cell-attracting chemokines, interferon-γ-inducible 10-kd protein (CXCL10) and monokine induced by interferon-γ (CXCL9), in the salivary gland lesions of patients with Sjögren's syndrome. Arthritis Rheum. 2002;46:2730-41.
27. Yanagawa K, Kawachi I, Toyoshima Y, Yokoseki A, Arakawa M, Hasegawa A et al. Pathologic and immunologic profiles of a limited form of neuromyelitis optica with myelitis. Neurology 2009;73:1628-37.
28. King LS, Agre P. Pathophysiology of the aquaporin water channels. Annu Rev Physiol 1996;58:619-48. Review.

29. Tsubota K, Hirai S, King LS, Aqre P, Ishida N. Defective cellular trafficking of lacrimal gland aquaporin-5 in Sjögren's syndrome. Lancet 2001;357:688-9.
30. Mavragani CP, Moutsopoulos HM. Sjögren's syndrome. Annu Rev Pathol 2014;9273-85.
31. Uzawa A, Masahiro M, Kuwabara S. Cytokines and chemokines in neuromyelitis optica: pathogenetic and therapeutic implications. Brain Pathology 2014;24:67-73.
32. Yamamura Y, Motegi K, Kani K, Takano H, Momota Y, Aota K et al. TNF-α inhibits aquaporin 5 expression in human salivary gland acinar cells via suppression of histone H4 acetylation. J Cell Mol Med 2012;16:1766-75.

Figure legends

Fig. 1. Expression of AQP4 in LSGs from patients with NMOsd or pSS.

Rabbit anti-AQP4 polyclonal antibody was used to detect the expression of AQP4. **A:** LSGs from a patient with typical pSS (SS5 in Table 2: Saxon test 0.99g/2min.) **B:** LSGs from an NMOsd-SS patient (NMOsd-SS4 in Table 2: Saxon test 0.68g/2min.). **C:** LSGs from a control (control2 in Table2: Saxon test 1.87g/2min). **D:** Human brain tissue was used as a positive control for AQP4. Hematoxylin was used for counterstaining (original magnification ×200).

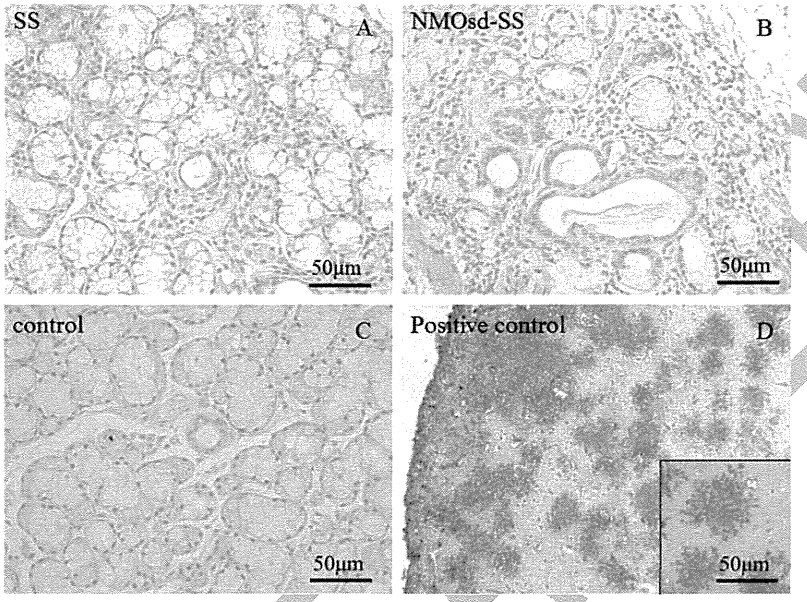

Fig. 2. Expression of AQP5 in LSGs from patients with NMOsd-SS or pSS.

Rabbit anti-AQP5 polyclonal antibody was used to detect the expression of AQP5. **A:** LSGs from a patient with typical pSS (SS2 in Table 2: Saxon test 0.27g/2min). **B:** LSGs from a patient with NMOsd-SS (NMOsd-SS1 in Table2 Saxon test 0.25g/2min). **C**: LSGs from a patient with NMOsd-SS (NMOsd-SS2 in Table2 Saxon test 1.17g/2min). **D**: LSGs from a patient with NMOsd-SS (NMOsd-SS3 in Table2 Saxon test 0.94g/2min.).**E:** LSGs from a control (Control2 in Table2: Saxon test 1.87g/2min). **F:** Human mandibular gland tissue was used as a positive control for AQP5. Haematoxylin was used for counterstaining (original magnification ×200).

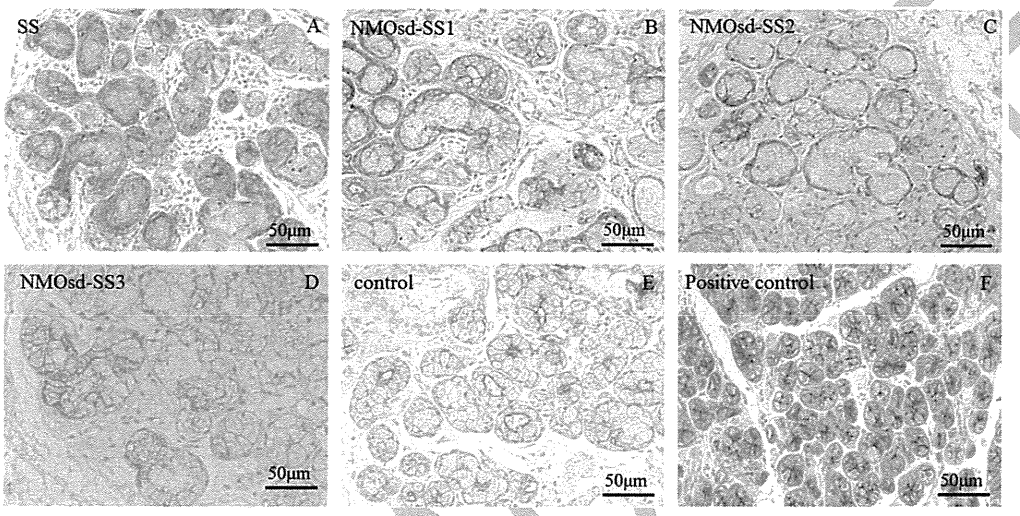

Fig. 3. Quantitative analysis of AQP5 in LSGs from patients with NMOsd-SS or pSS.

a: The immunostained specimens with AQP5 antibody were converted to gray scale, and we measured the average of the brightness of area in the acinus at the basement membrane side and gland luminal side. We examined the ratio of the brightness (gland luminal side/basement membrane side) with a calibration of the background brightness. Student's t-test was used. **b:** All subjects were divided into two groups depending on whether they scored above or < 1g/2min on the Saxon test, the brightness ratio was significantly higher in the < 1g/2min group. Squares, control. Circles, pSS. Triangles, NMOsd-SS.

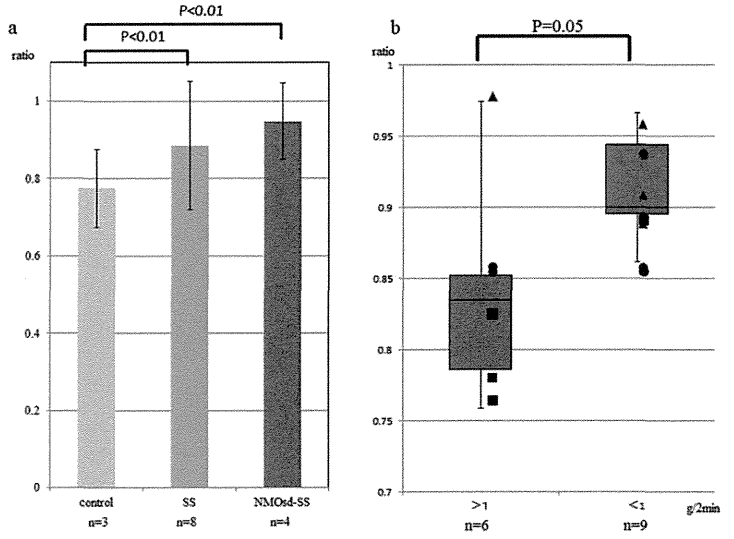

Fig. 4. Expression of TNF-□ and AQP5 in LSGs from patients with NMOsd-SS or SS.

a: Immunofluorescence staining of AQP5 in LSGs. The LSG tissues were double-labeled using mouse anti-TNF-□ antibody with FITC-conjugated secondary antibody (green) and rabbit anti-AQP5 antibody with TRITC-conjugated secondary antibody (red). The status of the nucleus was observed by Hoechst staining (blue). Representative results of three independent experiments with similar findings are shown. **b:** Expression AQP5 in SGECs under the presence of assigned concentrations of TNF-α and IL-10, determined by Western blotting. Vertical bars represent the ratio against □-actin bands. Mann-Whitney U-test. Results are from three independent experiments. In any groups, there was no significant difference as compared to control.

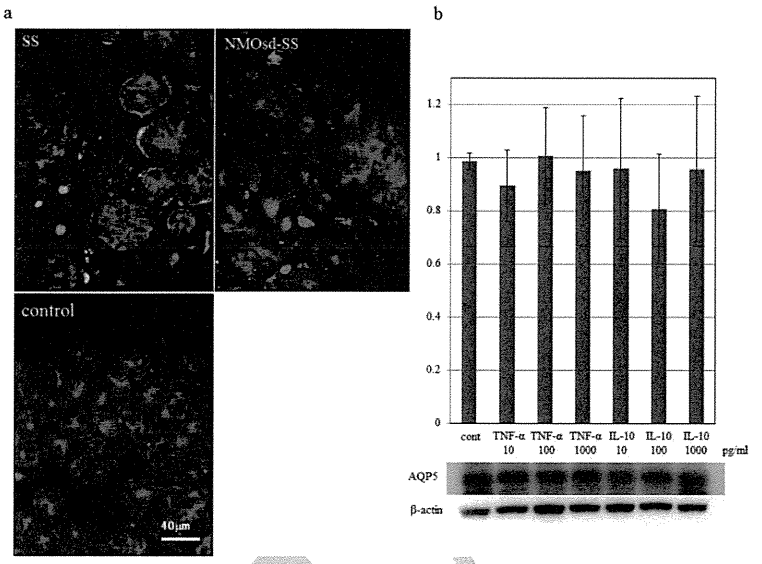

Table 1. The subjects' clinical manifestations

	NMOsd-SS n=4	Primary SS n=8	Control n=3	p-value
N (M/F)	4 (0/4)	8 (0/8)	3 (0/3)	
Age	58±8.0	56±12.9	45±7.4	0.87
Xerostomia	3/4	5/8	2/3	
Xerophthalmia	1/4	4/8	1/3	
Saxon test (g/2min)	0.76±0.34	0.77±0.56	2.0±0.50	0.98
Schirmer's test (ml/5min)	14.3±10.8	7.2±5.8	10.5±2.4	0.70
Anti-SS-A antibody	100%	100%	0%	0.28
Anti-SS-B antibody	0%	37.5%	0%	0.15
Rheumatoid factor	0%	75%	100%	0.048
IgG* (mg/dl)	1191.8±164.7	2620.5±891.9	1004.3±311.0	0.008
LSG biopsy grade	Grade 1 (2/4) Grade 2 (1/4) Grade 3 (1/4)	Grade 4 (8/8)	Grade 1 (2/2)	
Focus score average	0.25±0.43	5.75±2.3	0±0	0.004

Statistical differences between NMOsd-SS vs. pSS regarding age, the prevalence of anti-SS-A antibody, anti-SS-B antibody, IgG levels, and focus score (FS) ≥ 1[25] were calculated. Grading was as defined by Chisholm and Mason:[24] the presence of at least one focus of mononuclear cells per 4-mm^2 section presumes grade 3. The differences between NMOsd and SS data were calculated by Mann-Whitney U-test, respectively. *$p<0.05$.

Table 2. AQP4 and AQP5 immunostaining in labial salivary glands (LSGs)

	AQP4			AQP5			
	acinus	ducts	MNCs	acinus	Localization	ducts	MNCs
SS1	(−)	(−)	(−)	(+++)	homogenous	(−)	(−)
SS2	(−)	(−)	(−)	(+++)	homogenous	(−)	(−)
SS3	(−)	(−)	(−)	(+++)	homogenous	(−)	(−)
SS4	(−)	(−)	(−)	(+++)	homogenous	(−)	(−)
SS5	(−)	(−)	(−)	(+++)	homogenous	(−)	(−)
SS6	(−)	(−)	(−)	(+)	homogenous	(−)	(−)
SS7	(−)	(−)	(−)	(+++)	homogenous	(−)	(−)
SS8	(−)	(−)	(−)	(+++)	homogenous	(−)	(−)
NMOsd-SS1	(−)	(−)	(−)	(++)	homogenous ~BM	(−)	(−)
NMOsd-SS2	(−)	(−)	(−)	(+++)	BM	(−)	(−)
NMOsd-SS3	(−)	(−)	(−)	(+)	BM	(−)	(−)
NMOsd-SS4	(−)	(−)	(−)	(+)	homogenous	(−)	(−)
Control 1	(−)	(−)	(−)	(+++)	GL	(−)	NA

Control 2	(−)	(−)	(−)	(+++)	GL	(−)	NA
Control 3	(−)	(−)	(−)	(+++)	GL	(−)	NA

AQP4 was not stained in any tissue. AQP5 was expressed in acini. The localization of AQP5 was lost in the LSGs tissue of all of the NMOsd-SS and SS patients. Stained proportion with a salivary gland lobe was as follows; (−) 0-10%, (+) 10%–50%, (++) 50%–80%, (+++) >80%. NA: not available, MNCs: mononuclear cells, GL: gland luminal side, BM: basement membrane side, homogenous: cytoplasm was stained homogeneous

Japan College of Rheumatology
MODERN RHEUMATOLOGY

http://informahealthcare.com/mor
ISSN 1439-7595 (print), 1439-7609 (online)

Mod Rheumatol, 2016; 26(1): 99–104
© 2015 Japan College of Rheumatology
DOI: 10.3109/14397595.2015.1045256

informa
healthcare

ORIGINAL ARTICLE

Analysis of the downstream mediators of toll-like receptor 3-induced apoptosis in labial salivary glands in patients with Sjögren's syndrome

Yoshiro Horai[1], Hideki Nakamura[1], Yoshikazu Nakashima[1], Tomayoshi Hayashi[2], and Atsushi Kawakami[1]

[1]*Unit of Translational Medicine, Department of Immunology and Rheumatology, Nagasaki University Graduate School of Biomedical Sciences, Sakamoto, Nagasaki, Japan, and* [2]*Department of Pathology, Nagasaki Prefectural Shimabara Hospital, Shimabara, Nagasaki, Japan*

Abstract

Objectives. The aim of this study was to clarify the molecular mechanisms elicited by toll-like receptor (TLR)3 in salivary gland cell death in patients with SS.

Methods. Expression of TLR3 and its downstream molecules was examined by immunohistochemical analysis, immunofluorescence, Western blot (WB), and antibody dot-blot array in labial salivary glands (LSGs), and cultured primary salivary gland epithelial cells (SGECs) obtained from patients with SS. We also investigated the difference of expression between ducts/alveoli of LSGs and cultured SGECs.

Results. Phosphorylated Fas-associated protein with death domain (p-FADD) or caspase-8 was not found in ducts or alveoli of LSGs from SS patients and controls. Weak expression of receptor-interacting serine/threonine-protein kinase 3 (RIPK3) was found in SS patients, whereas no staining was observed in LSGs of controls. In contrast to LSGs, stimulation of SGECs with polyinosinic:cytidylic acid (poly I:C) significantly induced the expression of RIPK3, p-FADD, and cleaved caspase-8 by immunofluorescence and RIPK3, p-FADD, and cleaved caspase-3 by WB. However, it was counteracted by epidermal growth factor (EGF). Co-localization of anti-apoptotic molecules hemeoxygenase-2, heat shock protein 27, and p-protein kinase B or p-Akt was induced in EGF-stimulated SGECs.

Conclusions. We observed that poly I:C induced apoptosis of SGECs *in vitro* compared with a relatively low prevalence of apoptosis found in the ducts and alveoli of LSGs *in vivo*. Thus, we speculate that other counter-regulatory mechanisms, including those induced by EGF, might exist to protect against TLR3-mediated apoptosis of ductal and acinar epithelial cells *in vivo*.

Keywords

Apoptosis, Sjögren's syndrome, Toll-like receptor 3

History

Received 10 December 2014
Accepted 20 April 2015
Published online 28 May 2015

Introduction

Sjögren's syndrome (SS) is a chronic autoimmune disease characterized by sicca symptoms such as xerophthalmia and xerostomia [1]. Although the pathogenesis of SS has not been fully clarified, we observed a high prevalence of human T-cell leukemia virus type I (HTLV-I) infection among patients with SS in Nagasaki prefecture, a western Kyushu island of Japan, an endemic area of HTLV-I infection [2]. In this regard, toll-like receptors (TLRs), known as intermediation receptors preferentially involved in innate immunity, are expressed on ductal and acinar epithelial cells in labial salivary glands (LSGs) of SS, suggesting that TLR-related immune responses are associated with pathogenesis of SS [3].

TLR3 recognizes double-stranded RNAs, a marker of virus infection such as retroviruses, and transduces signals to cells following activation by the attachment of viruses [4,5]. We recently revealed that polyinosinic:cytidylic acid (poly I:C), a ligand for TLR3, induced the apoptotic cell death of cultured salivary gland epithelial cells (SGECs) by the activation of caspase-3 [6]. Since poly I:C induces the apoptosis of SGECs *in vitro* but in comparison there is a relatively low prevalence of apoptosis found in ducts and alveoli in LSGs *in vivo* [6], we speculate that counter-regulatory mechanisms exist to protect against TLR3-mediated apoptosis of SGECs *in vivo*. We previously reported epidermal growth factor (EGF)-mediated anti-apoptotic effects through activation of phosphoinositide 3-kinase–protein kinase B or PI3K–Akt and nuclear factor kappa B (NF-κB) [7]. Since the loss of ducts and alveoli is considered a major mechanism for salivary gland dysfunction of patients with SS, the molecular interactions elicited during TLR3 stimulation in SGECs may be crucial for the development of chronic sialadenitis.

In this study, we analyzed the signaling cascades of TLR3-mediated apoptosis interacting with EGF in SGECs from patients with SS.

Patients, materials, and methods

Patients

The study population for immunostaining consisted of 11 patients with SS (11 women, mean age: 57.0 years ± 14.0 SD, range: 19–78 years) and five controls (five women, mean age:

Correspondence to: Hideki Nakamura, Unit of Translational Medicine, Department of Immunology and Rheumatology, Nagasaki University Graduate School of Biomedical Sciences, 1-7-1 Sakamoto, Nagasaki 852-8501, Japan. Tel: + 81-92-819-7262. Fax: + 81-92-849-7270. E-mail: nhideki@nagasaki-u.ac.jp

53.6 years ± 14.7 SD, range: 34–77 years). A diagnosis of SS was based on the American-European Consensus Group (AECG) SS Classification Criteria of 2002 [8]. Control subjects had dry eye, dry mouth, or both, but had not fulfilled AECG SS Classification Criteria. All patients with SS revealed focal lymphocytic sialadenitis with a focus score ≥ 1 focus/4 mm^2 in LSGs biopsy, whereas mononuclear cell infiltration was not obvious in any of the five control subjects. Nine of eleven patients with SS were positive, whereas none of the five controls were positive for anti-SS-A antibodies. Blood specimens were obtained from all patients in this study for serological analysis, and were used to measure anti-SS-A antibody. In addition, all patients underwent LSGs biopsy under local anesthesia to assess the pathological findings of SS. All patients gave their informed consent to be subjected to the protocol, which was approved by the Institutional Ethics Committee of Nagasaki University.

Monoclonal and polyclonal antibodies

TLR3, RIPK3, phosphorylated Fas-associated protein with death domain (p-FADD), cleaved (cl) caspase 8, and cl caspase 3 in the LSGs were detected using antibodies listed in Table 1. Anti-TLR3 antibody was purchased from Santa Cruz Biotechnology (Santa Cruz, CA, USA), anti-RIPK3 was purchased from Epitomics Inc., (Burlingame, CA, USA), and antibodies to p-FADD, cl caspase 8, and cl caspase 3 were purchased from Cell Signaling Technology, Inc. (Beverly, MA, USA). Anti-β-actin and recombinant human EGF were purchased from Sigma (St Louis, MO, USA). Donkey anti-mouse immunoglobulin G (IgG) and rabbit polyclonal antibody, conjugated with peroxidase (for Western blotting), were purchased from MBL (Nagoya, Japan). Fluorescein isothiocyanate or FITC-conjugated donkey anti-mouse and tetramethyl rhodamine isothiocyanate or TRITC-conjugated donkey anti-rabbit, used for immunofluorescence, were purchased from Jackson Immunoresearch Laboratories Inc. (West Grove, PA, USA).

Culture of SGECs

LSGs obtained from incisional biopsies were washed with culture medium consisting of defined keratinocyte-SFM culture medium (Invitrogen Life Technologies, Carlsbad, CA, USA), penicillin–streptomycin, 0.4 μg/ml of hydrocortisone (Sigma), and 25 μg/ml of bovine pituitary extract (Kurabo, Osaka, Japan), excised with fine needles and scalpels, and the culture medium was replaced three times a week. Then, SGECs were cultured on six-well plates coated with type-I collagen (Iwaki, Tokyo, Japan).

After the outgrowth of SGECs reached confluence, they were subcultured into 100-mm^2 plates coated with type-I collagen. When SGECs reached confluence on the 100-mm^2 plates, they were cultured onto 60-mm^2 plates coated with type-I collagen. SGECs for immunofluorescence were subsequently distributed onto 12-mm^2 slips coated with type-I collagen, Cellmatrix (Nitta Gelatin, Inc., Osaka, Japan) in 24-well plates.

Immunohistochemical analyses of TLR3 and its downstream molecules in LSG biopsy specimens

We performed immunohistochemical staining to investigate the expression of TLR3 -associated molecules, EGF receptor (EGFR) and EGF *in vivo*. Briefly, endogenous peroxidase was inactivated by incubation with a 3% H_2O_2 solution after microwave epitope retrieval. The sections were then blocked with 5% normal horse serum, followed by incubation with monoclonal and polyclonal antibodies in a humid chamber for 60 min at room temperature. After incubation, all sections, including the negative control sections, were treated with peroxidase-conjugated secondary antibodies for 30 min (Histofine Simple Stain, Nichirei Biosciences, Tokyo, Japan). The color was developed by incubating the sections in 3,3'-diaminobenzidine or DAB and H_2O_2 for 10 min followed by counterstaining with hematoxylin solution. Prior to staining of salivary glands, we performed staining of hepatocellular carcinoma tissue purchased from ProSci Inc. (Poway, CA, USA) to set up optimal staining conditions.

Immunofluorescence

We performed immunofluorescence to investigate TLR3-associated molecular mechanisms *in vitro*. SGECs distributed onto 12-mm^2 slips coated with Cellmatrix were incubated for 24 h in either the presence or absence of 50 ng/ml of EGF and/or poly I:C after 24-h starvation of growth supplement. EGF and poly I:C were administered at the same time. SGECs were then fixed in 4% paraformaldehyde immersed in methanol at −20°C for 10 min.

Western blotting

Western blot (WB) analysis was performed as described previously [9]. After SGEC lysis and measuring protein concentrations, identical amounts of protein were subjected to 12.5% sodium dodecyl sulfate-polyacrylamide gel electrophoresis. The proteins were transferred to a polyvinylidene fluoride filter and blocked for 1 h with 5% nonfat dried milk in Tris-buffered saline containing 0.1%

Table 1. Antibodies used in the study.

Antibodies	Immunogen	Poly/mono	Working dilution	Application	Source
TLR3	TLR3 of human	Poly	1:100	IHC, IF, WB	Goat
RIPK3	N-terminus of human RIPK3	Poly	1:100	IHC, IF, WB	Rabbit
p-FADD	Ser^{194} of human FADD	Poly	1:100–1:1,000	IHC, IF, WB	Rabbit
Cl caspase 8	Cl caspase 8 of human	Mono	1:100–1:1,000	IHC, IF, WB	Rabbit
Cl caspase 3	Asp^{175} of human cl caspase 3	Mono	1:100–1:1,000	IF, WB	Rabbit
EGFR	EGFR of human	Poly	1:50	IHC	Rabbit
EGF	EGF of human	Mono	1:500	IHC	Mouse
HO-2	HO-2 of human	Mono	1:150	IHC, IF	Mouse
HSP27	HSP-27 of human	Mono	1:100	IHC, IF	Mouse

TLR3 Toll-like receptor 3, *RIPK3* Receptor-interacting serine/threonine protein kinase 3, *p-FADD* Phosphorylated Fas-associated protein with death domain, *cl caspase 8* Cleaved caspase 8, *cl caspase 3* Cleaved caspase 3, *EGFR* Epidermal growth factor receptor, *EGF* Epidermal growth factor, *HO-2* hemeoxygenase-2, *HSP27* heat shock protein 27, *Poly* Polyclonal antibody, *Mono* Monoclonal antibody, *IHC* Immunohistochemistry, *IF* Immunofluorescence, *WB* Western blot.

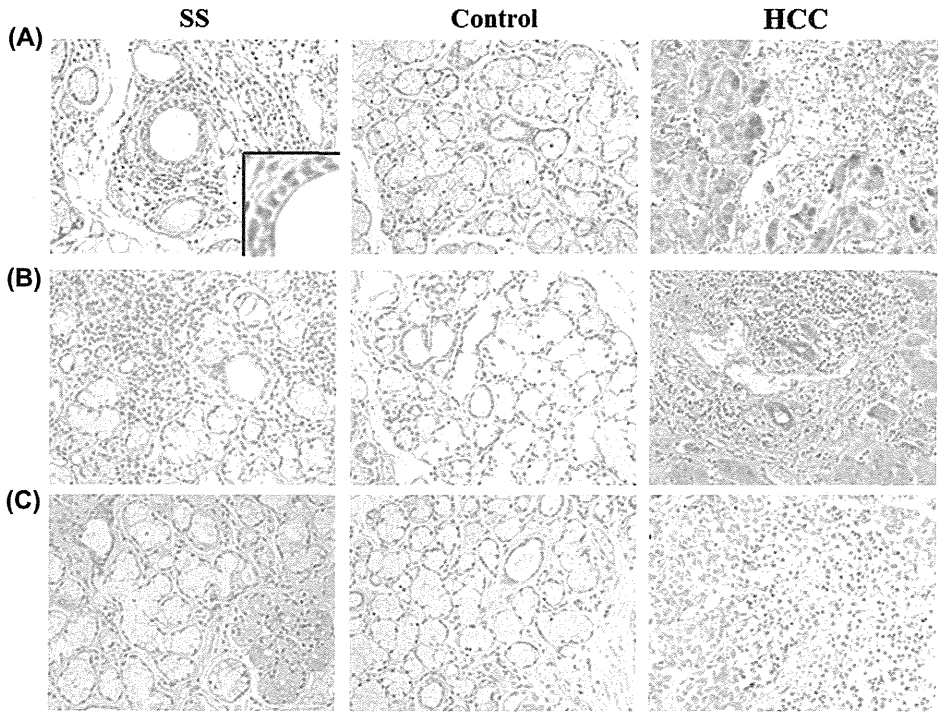

Figure 1. Representative immunostaining images of TLR3 downstream molecules in salivary glands from SS patients. *HCC* hepatocellular carcinoma (positive control). (A) RIPK3: mild staining of ducts and alveoli was detected, whereas no staining was present in controls. Inset shows representative staining of RIPK3. (B) p-FADD: staining for p-FADD was not present in SS or control tissues. (C) cl caspase 8: staining for cl caspase 8 was not apparent in SS or control tissues.

Tween 20 (TBST). Then, membranes were incubated in a 1:100 dilution of rabbit anti-receptor-interacting serine/threonine protein kinase 3 (RIPK3) polyclonal antibody, a 1:1,000 dilution of rabbit anti-p-FADD polyclonal antibody, a 1:1,000 dilution of rabbit anti-cl caspase 8 monoclonal antibody and a 1:1000 dilution of rabbit anti-cl caspase 3 monoclonal antibody at 4°C overnight. The membrane was washed with TBST and incubated with a 1:1000 dilution of donkey anti-rabbit IgG coupled with horseradish peroxidase, after which detection was performed using Amersham Hyperfilm ECL (GE Healthcare UK Ltd, Little Chalfont, UK). We performed WB analysis of samples obtained from three different patients to clarify increased expression of cl caspase 3 after stimulation with poly I:C. The density of the bands was captured and measured by ImageJ and developed at the National Institutes of Health to measure pixel intensity. The difference between the two groups (poly I:C− and poly I:C+) was determined by Student's *t*-test.

Apoptosis dot-blot array analysis

The analysis of apoptosis-related molecules was performed with R&D Systems' Human Apoptosis Array Kit following the manufacturer's instructions. Briefly, diluted co-cultured cellular extracts were incubated on membranes for 2 h after a 2-h incubation, and a cocktail of biotinylated antibodies was added to the membranes and incubated for 1 h on a rocking platform shaker. Chemiluminescent reagents were then used after incubation with streptavidin–horseradish peroxidase for 30 min. The expressions are represented as the ratio compared with control dot-blots. We used ImageJ to measure pixel intensity.

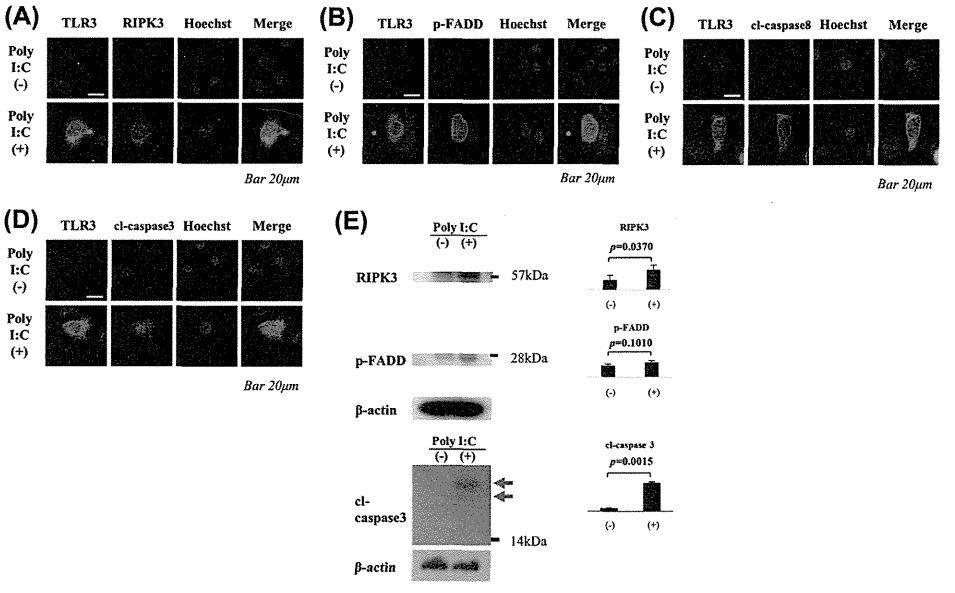

Figure 2. Immunofluorescent detection of TLR3 downstream molecules following 24 h poly I:C stimulation in vitro. (A) RIPK3: Increased expression of RIPK3 was observed. (B) p-FADD: Increased expression of p-FADD was observed in contrast to the immunostaining results. (C) cl caspase 8: Increased expression of cl caspase 8. (D) cl caspase 3: Increased expression of cl caspase 3. (E) WB analysis of RIPK3, p-FADD, and cl caspase 3: increased expressions of RIPK3 with statistical significance, p-FADD with a tendency toward statistical significance and cl caspase3 with statistical significance To identify and evaluate the differences between density of bands with and without poly I:C stimulation, we used variables which were calculated using the density ratios of RIPK3, p-FADD, or cl caspase 3 to β-actin. Values of $p < 0.05$ were considered significant.

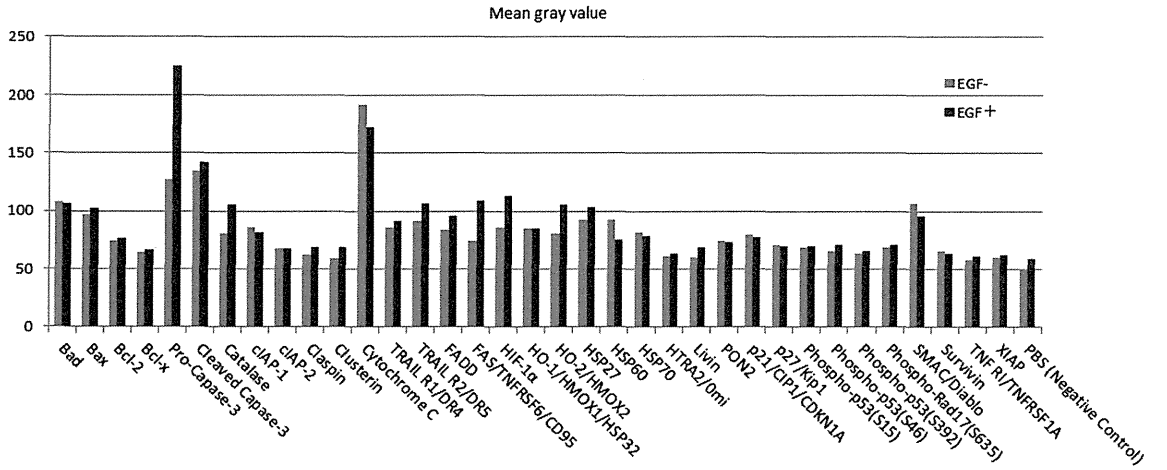

Figure 3. Pro- and anti-apoptotic molecules in apoptosis antibody array in the presence and absence of EGF. Increased expression of several anti-apoptotic molecules, HO-2 and HSP 27, and several apoptotic molecules such as pro-caspase 3, FADD, and Fas was observed in the presence of EGF.

Results

Immunohistochemical detection of RIPK3, p-FADD, and cl caspase 8

RIPK3 was weakly observed in ducts and alveoli from SS, whereas no staining was observed in LSGs from controls (Figure 1A). In contrast, p-FADD or cl caspase 8 staining was not detected in LSGs from SS patients or controls (Figure 1B, C).

In vitro detection of RIPK3, p-FADD, cl caspase 8, and cl caspase 3 in SGECs

As previously reported [3], TLR3 was expressed in ducts/alveoli of both LSGs (data not shown) and primary SGECs (Figure 2A–D). RIPK3 and p-FADD were not expressed in unstimulated SGECs (Figure 2A and B). Accordingly, neither cl caspase-8 nor cl caspase-3 was detected in unstimulated SGECs (Figure 2C–E). Triggering TLR3 with poly I:C significantly increased the expression of RIPK3, p-FADD, cl caspase 8, and cl caspase 3 in SGECs (Figure 2A–D). Increased expressions of RIPK3 with statistical significance, p-FADD with a tendency toward statistical significance, and cl caspase 3 with statistical significance after poly I:C stimulation were also observed in WB (Figure 2E). The expression of TLR3 itself was also increased in SGECs following poly I:C incubation (Figure 2A–D).

Modulation of TLR3-mediated effects by EGF in SGECs

Expression patterns of TLR3 and its related molecules in unstimulated SGECs resembled those in LSGs of SS patients, whereas the triggering of TLR3 induced the opposite phenotypes. These data indicate that some humoral factors might interfere with TLR3-mediated effects *in vivo*. One such alteration could be induced by EGF as it is expressed in the LSGs of SS patients and acts as a growth or anti-apoptotic factor for ductal epithelial cells [7]. Therefore, we measured changes of apoptosis-related molecules in SGECs induced by EGF using a dot-blot array assay kit. Increased expression of several anti-apoptotic molecules, such as hemeoxygenase-2 (HO-2) and heat shock protein 27 (HSP27)

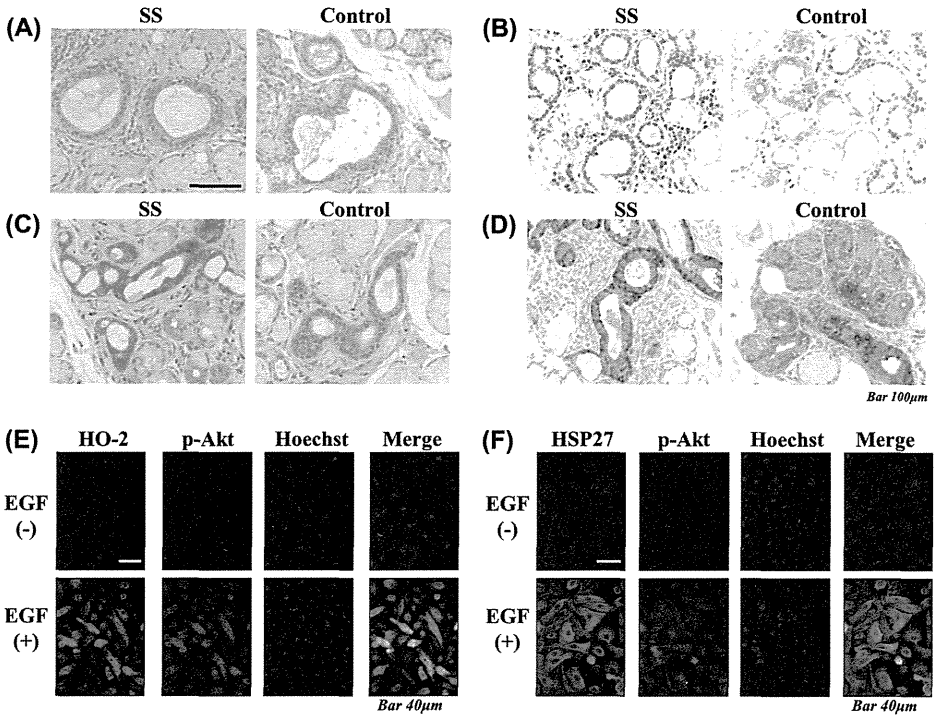

Figure 4. Expression of EGFR in LSGs and EGF-induced molecules in SGECs. (A) Immunostaining images of whole EGFR in salivary glands from SS and control: staining of ducts was detected in LSG of SS as well as control. (B) Immunostaining images of EGF in salivary glands from SS and control: staining of ducts was detected in LSG of SS as well as control. (C) Relatively more increased expression of HO-2 was observed in LSG of SS than in control. (D) Relatively more increased expression of HSP27 was observed in LSG of SS than in control. Immunofluorescent detection of co-expression of p-Akt and anti-apoptotic molecules identified by apoptosis antibody array. SGECs were stimulated with 50 ng/ml of EGF for 24 h. The nuclei were stained blue with Hoechst 33258 to clarify distribution of p-Akt and presented as a merged view with p-Akt. (E) Co-expression of p-Akt and HO-2 was shown. (F) Co-expression of p-Akt and HSP-27 was shown.

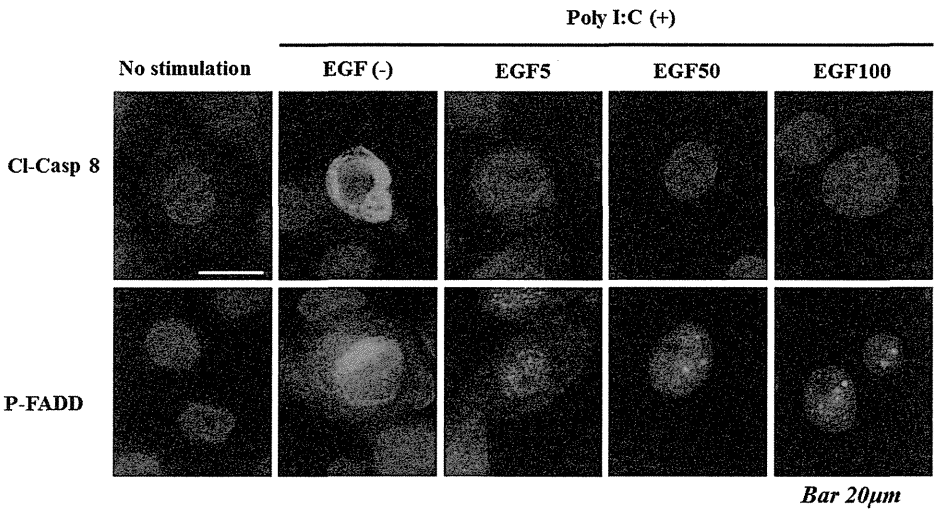

Figure 5. Effect of EGF on poly I:C-induced cl caspase 8 and p-FADD 24-h stimulation of SGECs from SS patients with poly I:C induced the expression of cl caspase 8 and p-FADD, which is inhibited dose-dependently by the addition of EGF (0–50 ng/ml). The nuclei were stained with Hoechst 33258 to clarify distribution of SGECs presented as a merged view with cl caspase 8 or p-FADD.

and several apoptotic molecules such as pro-caspase 3, FADD, and Fas, was observed after stimulation with EGF (Figure 3).

Whole EGFR (Figure 4A) and EGF (Figure 4B) were observed in ducts of SS as well as controls. Relatively more increased expressions of HO-2 (Figure 4C) and HSP27 (Figure 4D) were observed in LSG of SS than in control. Immunostaining after stimulation with EGF revealed co-expression of phosphorylated-Akt (p-Akt) with HO-2 or HSP27 (Figure 4E and F). Although stimulation of SGECs with poly I:C induced the expression of cl caspase 8 and p-FADD with nuclear fragmentation, which was compatible with poly I:C-induced apoptosis. EGF dose-dependently inhibited the expression of these molecules (Figure 5) and nuclear fragmentation induced by poly I:C.

Discussion

TLR3 recognizes dsRNA derived from many viruses or poly I:C, and triggers the production of type-I interferon [10]. Recent studies have suggested that TLR3 signaling has important roles in immune responses against viral infections, as well as apoptosis in cancer and autoimmune diseases [11,12].

Numerous molecules involved in the apoptosis of LSGs in SS patients have been reported [13]. We found that cultured SGECs were committed to apoptosis by Fas or tumor necrosis factor-related apoptosis-inducing ligand (TRAIL); however, the participation of downstream molecules is different for each apoptotic process of SGECs triggered by Fas or TRAIL [9].

Our recent study revealed that the triggering of TLR3 by poly I:C in SGECs activated caspase-3. Salaun et al. also demonstrated that poly I:C stimulation induced apoptosis mediated by TLR3 in human breast cancer cells [11], in which activation of TIR domain containing adapter inducing interferon-β (TRIF) was involved. Khvalevsky et al. described that TLR3 signaling induced cytokine production and apoptosis via activation of caspase 8 in human hepatocellular carcinoma cells [12]. Considering the putative implication of TLR3 in the pathogenesis of SS, we focused on the regulatory mechanisms of TLR3-mediated apoptosis of SGECs in the present study.

The present study suggests that TLR3-induced apoptosis of SGECs was mediated through FADD/caspase-8/caspase-3 pathways. Furthermore, it is interesting to note that the signaling cascades elicited from TLR3 together with EGF *in vitro* may reflect the expression pattern of RIPK3, FADD, caspase-8, and caspase-3 of SGECs *in vivo*. Our previous studies demonstrating the strong expression of TLR3, EGFR, and phosphorylated EGFR [6,7] may support this speculation. We also recently showed that Akt, activated by EGF, acts as an anti-apoptotic molecule during TLR3-mediated apoptosis of SGECs. Furthermore, our present study suggests that other anti-apoptotic molecules, including HO-2 or HSP27, function synergistically with Akt against TLR3-mediated apoptosis because the expression of HO-2 and HSP27 was augmented and co-localized in SGECs with p-Akt by EGF. Since EGFR constitutively expressed on ducts in LSGs (Figure 4A), it was presumed that EGF exerted to induce functional HO-2 or HSP27 in SGECs. Co-localization of HO-2 or HSP-27 with Akt was observed in other cell types during anti-apoptotic processes [14,15]. In Figure 3, several apoptotic molecules such as pro-caspase 3, FADD, and Fas seemed to be increased after stimulation with EGF, in addition to HO-2 and HSP27. As we described previously, apoptotic cell death was observed in SS [6]. In this study, some extent of cell death was observed in the course of subculture. Based on these findings, it is presumed that HO-2 and HSP27 antagonize the apoptotic mechanism in SS.

Infection with viruses thought to be involved in SS etiology, such as HTLV-I and Epstein–Barr virus, have been found in the salivary glands of SS patients [2,16]. In addition, SS-A/Ro, which is recognized by anti SS-A/Ro antibodies, includes small RNA particles [17,18]. Since TLR3 recognizes RNA molecules [19], these RNA viruses and RNA particles might be involved in the pathogenesis of SS through TLR3. Although poly I:C preferentially triggers apoptotic processes in SGECs, other TLR3 ligands might induce pro-inflammatory reactions because TLR3 was originally identified as activating interferon regulatory factors (IRFs) and NF-κB [19]. Therefore, the role of TLR3 in facilitating the chronic sialadenitis of SS patients remains to be elucidated.

This is the first study investigating the downstream molecular pathways of TLR3-controlled cell death of SGECs in SS patients. The balance between TLR3-induced activation of caspase cascades and tropic actions against apoptosis might compete *in situ* in salivary glands. Future studies are required to understand fully TLR-mediated cell death pathways and their detailed mechanisms.

Acknowledgements

We thank Yoshiko Takahashi (Nagasaki University) for her excellent technical assistance.

Funding

This work was supported in part by a Grant from the Ministry of Health, Labour and Welfare, Japan.

Conflict of interest

None.

References

1. Moutsopoulos HM, Chused TM, Mann DL, Klippel JH, Fauci AS, Frank MM, et al. Sjögren's syndrome (Sicca syndrome): Current issues. Ann Intern Med. 1980;92(2 Pt 1):212–26.
2. Terada K, Katamine S, Eguchi K, Moriuchi R, Kita M, Shimada H, et al. Prevalence of serum and salivary antibodies to HTLV-1 in Sjögren's syndrome. Lancet. 1994;344(8930):1116–9.
3. Kawakami A, Nakashima K, Tamai M, Nakamura H, Iwanaga N, Fujikawa K, et al. Toll-like receptor in salivary glands from patients with Sjögren's syndrome: Functional analysis by human salivary gland cell line. J Rheumatol. 2007;34(5):1019–26.
4. Vercammen E, Staal J, Beyaert R. Sensing of viral infection and activation of innate immunity by toll-like receptor 3. Clin Microbiol Rev. 2008;21(1):13–25.
5. Lai Y, Yi G, Chen A, Bhardwaj K, Tragesser BJ, Valverde RA, et al. Viral double-strand RNA-binding proteins can enhance innate immune signaling by toll-like Receptor 3. PLOS ONE. 2011;6:e25837.
6. Nakamura H, Horai Y, Suzuki T, Okada A, Ichinose K, Yamasaki S, et al. TLR3-mediated apoptosis and activation of phosphorylated Akt in the salivary gland epithelial cells of primary Sjögren's syndrome patients. Rheumatol Int. 2013;33(2):441–50.
7. Nakamura H, Kawakami A, Ida H, Koji T, Eguchi K. EGF activates PI3K-Akt and NF-kappaB via distinct pathways in salivary epithelial cells in Sjögren's syndrome. Rheumatol Int. 2007;28(2):127–36.
8. Vitali C, Bombardieri S, Jonsson R, Moutsopoulos HM, Alexander EL, Carsons SE, et al. Classification criteria for Sjögren's syndrome: a revised version of the European criteria proposed by the American-European Consensus Group. Ann Rheum Dis. 2002;61(6):554–8.
9. Nakamura H, Kawakami A, Iwamoto N, Ida H, Koji T, Eguchi K. Rapid and significant induction of TRAIL-mediated type II cells in apoptosis of primary salivary epithelial cells in primary Sjögren's syndrome. Apoptosis. 2008;13(11):1322–30.
10. Alexopoulou L, Holt AC, Medzhitov R, Flavell RA. Recognition of double-stranded RNA and activation of NF-kappaB by toll-like receptor 3. Nature. 2001;413(6857):732–8.
11. Salaun B, Coste I, Rissoan MC, Lebecque SJ, Renno T. TLR3 can directly trigger apoptosis in human cancer cells. J Immunol. 2006;176(8):4894–901.
12. Khvalevsky E, Rivkin L, Rachmilewitz J, Galun E, Giladi H. TLR3 signaling in a hepatoma cell line is skewed towards apoptosis. J Cell Biochem. 2007;100(5):1301–12.
13. Mitsias DI, Kapsogeorgou EK, Moutsopoulos HM. The role of epithelial cells in the initiation and perpetuation of autoimmune lesions: Lessons from Sjögren's syndrome (autoimmune epithelitis). Lupus. 2006;15(5):255–61.
14. Turkseven S, Drummond G, Rezzani R, Rodella L, Quan S, Ikehara S, Abraham NG. Impact of silencing HO-2 on EC-SOD and the mitochondrial signaling pathway. J Cell Biochem. 2007;100(4):815–23.
15. Son TW, Yun SP, Yong MS, Seo BN, Ryu JM, Youn HY, et al. Netrin-1 protects hypoxia-induced mitochondrial apoptosis through HSP27 expression via DCC- and integrin α6β4-dependent Akt, GSK-3β, and HSF-1 in mesenchymal stem cells. Cell Death Dis. 2013;4(3):e563.
16. Saito I, Shimuta M, Terauchi K, Tsubota K, Yodoi J, Miyasaka N. Increased expression of human thioredoxin/adult T cell leukemia-derived factor in Sjögren's syndrome. Arthritis Rheum. 1996;39(5):773–82.
17. Franceschini F, Cavazzana I. Anti-Ro/SSA and La/SSB antibodies. Autoimmunity. 2005;38(1):55–63.
18. Rader MD, O'Brien C, Liu YS, Harley JB, Reichlin M. Heterogeneity of the Ro/SSA antigen. Different molecular forms in lymphocytes and red blood cells. J Clin Invest. 1989;83(4):1293–8.
19. Takeda K, Akira S. TLR signaling pathways. Semin Immunol. 2004;16(1):3–9

ARTHRITIS & RHEUMATOLOGY
Vol. 67, No. 4, April 2015, pp 1096–1106
DOI 10.1002/art.39009

Direct Infection of Primary Salivary Gland Epithelial Cells by Human T Lymphotropic Virus Type I in Patients With Sjögren's Syndrome

Hideki Nakamura,[1] Yoshiko Takahashi,[1] Tomomi Yamamoto-Fukuda,[1] Yoshiro Horai,[1] Yoshikazu Nakashima,[1] Kazuhiko Arima,[1] Tatsufumi Nakamura,[2] Takehiko Koji,[1] and Atsushi Kawakami[1]

Objective. **To investigate whether human T lymphotropic virus type I (HTLV-I) directly infects salivary gland epithelial cells (SGECs) and induces the niche of the salivary glands in patients with Sjögren's syndrome (SS).**

Methods. **SGECs were cultured with the HTLV-I–producing CD4+ T cell line HCT-5 or with Jurkat cells. Antibody arrays, immunofluorescence analysis, and enzyme-linked immunosorbent assay (ELISA) were used to determine the profiles of inflammation-related molecules, and the profiles of apoptosis-related molecules were determined by antibody array and immunofluorescence analysis. The presence of HTLV-I–related molecules was assessed by immunofluorescence analysis and in situ polymerase chain reaction. Apoptosis of SGECs was evaluated by TUNEL staining.**

Results. **Among the SGECs, 7.8 ± 1.3% (mean ± SD) were positive for HTLV-I–related proteins after 96-hour coculture with HCT-5 cells. Nuclear NF-κB p65 was also detected in 10% of the SGECs. The presence of HTLV-I proviral DNA in SGECs after coculture with HCT-5 cells was detected by in situ polymerase chain reaction. After coculture of SGECs with HCT-5, the expression of cytokines and chemokines, including soluble intercellular adhesion molecule 1, RANTES, and interferon γ–induced protein 10 kd (IP-10/CXCL10) was increased in a time-dependent manner. The expression of proapoptotic molecules (e.g., cytochrome c and Fas) and antiapoptotic molecules (e.g., Bcl-2, Heme oxygenase 2, and Hsp27) was increased in the SGECs cocultured with HCT-5, showing that apoptosis of SGECs was not detected after coculture with HCT-5 or Jurkat cells.**

Conclusion. **HTLV-I is thought to infect SGECs and alter their cellular functions. These changes may induce the niche of SS and contribute to the development of SS in anti–HTLV-I antibody–positive individuals.**

Human T lymphotropic virus type I (HTLV-I) has been reported to be involved in the pathogenesis of primary Sjögren's syndrome (SS) in endemic areas, including Nagasaki City, Japan (1–3). The extremely high prevalence of SS among patients with HTLV-I–associated myelopathy (HAM) appears to confirm a strong relationship between HTLV-I infection and SS (4–6). A previous study by our group also revealed the clinical characteristics of anti–HTLV-I antibody–positive SS patients and showed that the labial salivary glands (LSGs) of such patients are not destructible compared with the LSGs of anti–HTLV-I antibody–negative patients with SS (7). In addition, the low prevalence of ectopic germinal centers (GCs) as well as the low expression of CXCL13 in infiltrating mononuclear cells in LSGs were shown to be immunohistologic characteristics of anti–HTLV-I antibody–positive patients with SS (8).

HTLV-I preferentially infects T cells, especially CD4+ T cells, and the observations described above indicate that the T cell lineage may primarily contribute

Supported in part by a grant from the Ministry of Health, Labor, and Welfare, Japan.

[1]Hideki Nakamura, MD, PhD, Yoshiko Takahashi, MD, Tomomi Yamamoto-Fukuda, MD, PhD, Yoshiro Horai, MD, Yoshikazu Nakashima, MD, Kazuhiko Arima, MD, PhD, Takehiko Koji, PhD, Atsushi Kawakami, MD, PhD: Nagasaki University Graduate School of Biomedical Sciences, Nagasaki, Japan; [2]Tatsufumi Nakamura, MD, PhD: Nagasaki International University, Nagasaki, Japan.

Address correspondence to Hideki Nakamura, MD, PhD, Unit of Translational Medicine, Department of Immunology and Rheumatology, Nagasaki University Graduate School of Biomedical Sciences, 1-7-1 Sakamoto, Nagasaki City, Nagasaki 852-8501, Japan. E-mail: nhideki@nagasaki-u.ac.jp.

Submitted for publication April 27, 2014; accepted in revised form December 19, 2014.

to the pathogenesis of anti–HTLV-I antibody–positive SS. However, cell types other than T cells, including the human retinal pigment epithelial cell line ARPE-19 (9), and human primary fibroblast-like synoviocytes (FLS) (10) were reported to be susceptible to HTLV-I infection. In ARPE-19 cells, the expression of intercellular adhesion molecule 1 (ICAM-1) is increased by HTLV-I, and the production of granulocyte–macrophage colony-stimulating factor (GM-CSF) from FLS is induced by HTLV-I.

These observations suggested that HTLV-I may infect cell lineages other than T cells in human salivary glands and may contribute to the development of SS. In this regard, ductal epithelial cells are considered candidate cells, because various cytokines, chemokines, and apoptosis-related molecules have been shown to be expressed in these cells (1). In addition, ductal epithelial cells attract T cells into the salivary glands of patients with SS through production of interferon-γ (IFNγ)–inducible 10-kd protein (IP-10; CXCL10) and monokine induced by IFNγ (CXCL9) (11).

In the current study, we investigated whether HTLV-I infects human primary salivary gland epithelial cells (SGECs) and modulates the production of functional molecules.

PATIENTS AND METHODS

Patients. Primary SGECs were obtained from the LSGs of 15 female patients with primary SS (mean ± SD age 53.2 ± 15.4 years). In all patients, SS was diagnosed according to the revised criteria proposed by the American–European Consensus Group (12), and anti–HTLV-I antibodies were absent, as measured by chemiluminescent enzyme immunoassay.

Antibodies and reagents. Mouse anti–HTLV-I antibodies (p19, p38, and Gag) were obtained from Chemicon, and mouse anti–NF-κB p65 antibody, mouse anti–cytochrome c antibody, mouse anti-Hsp27 antibody, and rabbit anti-Fas antibody were obtained from Santa Cruz Biotechnology. Mouse anti–heme oxygenase 2 (anti–HO-2) antibody was purchased from OriGene, and rabbit anti–ICAM-1 antibody, rabbit anti–growth-related oncogene (anti-GRO)/CXCL1 antibody, anti-CCL5/RANTES antibody, and rabbit anti–IP-10/CXCL10 antibody were purchased from LifeSpan Biosciences. Rabbit anti–interleukin-8 (anti–IL-8) antibody was purchased from ABgene. Secondary antibodies, including fluorescein isothiocyanate (FITC)–conjugated donkey anti-mouse IgG and tetramethylrhodamine isothiocyanate (TRITC)–conjugated donkey anti-rabbit IgG, were purchased from Jackson ImmunoResearch. Hoechst 33258 was purchased from Sigma. A Proteome Profiler Human Cytokine Array Kit, Panel A, and a Quantikine ELISA kit for soluble ICAM-1 (sICAM-1), CXCL10/IP-10, CCR5/RANTES, CXCL1/GROα, and CXCL8/IL-8 were purchased from R&D Systems. Cy3–dUTP was purchased from GE Healthcare. Monoclonal mouse anti-human CD4, anti-human CD8, anti-human CD20cy, mouse IgG1, and monoclonal rabbit anti-human cytokeratin 8/18 antibodies were purchased from Dako.

LSG biopsy and cell culture. Each patient underwent a lower lip salivary gland biopsy under local anesthesia. Some of the specimens were stained with hematoxylin to diagnose sialadenitis, and some were used for culture of SGECs in a defined keratinocyte–serum-free medium (SFM) (Invitrogen Life Technologies) supplemented with hydrocortisone (Sigma) and bovine pituitary extract (Kurabo). In all 15 patients, the diagnosis of SS was compatible with the Chisholm and Mason scale for histologic grading of LSG biopsy tissue (13).

For the coculture of SGECs with HTLV-I–producing T cells, HCT-5 cells (which are derived from the cerebrospinal fluid cells of patients with HAM [14]), were cultured with SGECs for the designated period of time in defined keratinocyte–SFM culture medium. As a control toward HCT-5, the non–HTLV-I–infected T cell line Jurkat was cultured in RPMI 1640 medium with 10% fetal bovine serum. For the experiments described below, HCT-5 or Jurkat cells were cocultured (2:1) with SGECs at the time when the cells were seeded. Briefly, the SGECs were seeded onto sterile coverslips for immunofluorescence analysis. Next, HCT-5 cells were added 24 hours after the SGECs attached to and grew on the coverslips. For immunofluorescence analysis, the cells were stringently washed with phosphate buffered saline (PBS) to remove any remaining HCT-5 cells. Informed consent for the use of LSG biopsy samples was obtained from all 9 patients at the commencement of the study. The study was conducted with the approval of the human ethics committee at Nagasaki University Hospital.

Immunofluorescence analysis. Immunofluorescence analyses were performed as previously described (15). Briefly, SGECs cultured on 12-mm^2 coverslips were fixed in PBS containing 4% paraformaldehyde (PFA) at 4°C, followed by immersion in methanol at −20°C for 10 minutes. After fixation, the SGECs were blocked in 5% normal horse serum in PBS and then incubated with the primary antibodies for 1 hour at room temperature, followed by incubation with FITC-conjugated and TRITC-conjugated secondary antibodies and Hoechst 33258, in the dark. The SGECs were then mounted in Vectashield mounting medium (Vector) and scanned with a fluorescence microscope (BIOREVO BZ-9000; Keyence). To measure the immunofluorescence of the HCT-5 cells, fixed cells were incubated with mouse primary monoclonal antibodies as cell surface markers, followed by FITC-conjugated secondary antibody and Hoechst 33258. Control experiments were performed to confirm the isotype specificity of the secondary antibodies. Immunostaining of HCT-5 cells was performed in the same manner as that described above for SGECs.

TUNEL staining. To investigate DNA double-strand breaks in SGECs, TUNEL staining was performed as described in a previous study by our group (16). After fixation, SGECs were incubated in 4% PFA at 4°C for 15 minutes, followed by immersion in PBS with 0.5% Tween 20 and 0.2% bovine serum albumin, using a MEBSTAIN Apoptosis Kit Direct (MBL). The SGECs were then incubated with a 50-μl terminal deoxynucleotidyl transferase solution at 37°C for 1 hour. The dUTP signal as detected by FITC was captured using a BIOREVO BZ-9000 fluorescence microscope (Keyence). TRAIL was used as a positive control to show induction of apoptosis (15).